

PROPAGATION CHARACTERISTICS IN THE EARTH-  
IONOSPHERE WAVEGUIDE FOR VLF WAVES  
EMITTED FROM TRAPPING CONES AT  
HIGH LATITUDES

Isamu NAGANO<sup>1</sup>, Masayoshi MAMBO<sup>1</sup>, Tetsuya SHIMBO<sup>1</sup>  
and Iwane KIMURA<sup>2</sup>

<sup>1</sup>*Department of Electrical Engineering and Computer Science, Kanazawa  
University, 40–20 Kodatsuno 2-chome, Kanazawa 920*

<sup>2</sup>*Department of Electrical Engineering II, Kyoto University,  
Yoshida Honmachi, Sakyo-ku, Kyoto 606*

**Abstract:** It is important to clarify the relationship between VLF-ELF wave characteristics on the ground and in the ionosphere for a comprehensive understanding of the ground-based observation data. In this paper, the amplitude and polarization of VLF waves at various places on the ground are calculated with an ionospheric model at high latitudes, through a full wave technique when various size of trapping cones are existing. Some results of the numerical calculation are presented. Major results are as follows: (1) Waves with an amplitude within 12 dB of the maximum intensity are found in an area of 300 km (east-west direction)  $\times$  400 km (north-south direction) when some part of the trapping cone overlaps with the transmission cone. (2) The left-handed polarization wave can exist even within a distance of 100 km from the point of maximum intensity, where the intensity is as strong as  $\sim -10$  dB of the maximum intensity.

## 1. Introduction

It is well-known from Snell's law that the downgoing whistler wave can penetrate the lower ionosphere when the wave normal lies within a transmission cone (HELLIWELL, 1965). Computer programs for solving the one dimensional wave equation have been developed with the aid of digital computers (BUDDEN, 1961), and the transmission and reflection coefficients from the bottom side of the ionosphere have been studied for plane waves (PITTEWAY and JESPERSEN, 1966; TSURUDA, 1973). On the other hand, multi-point conjugate observations of the signal from the VLF transmitter located at Siple Station, Antarctica have been carried out in Canada by TSURUDA *et al.* (1982). They reported that the Siple signals propagated to the northern hemisphere in the whistler mode and had an amplitude distribution on the ground with a spatial attenuation rate as high as 6 dB/100 km from the peak level.

NAGANO *et al.* (1982) calculated the wave intensity and polarization pattern on the ground with an assumption that one dimensional beam of VLF wave was injected from the upper ionosphere. They obtained a spatial attenuation of  $-10$  dB/100 km, which was consistent with the value described above. Furthermore, NAGANO *et al.* (1986) (to be referred to as "paper 1" hereafter in this paper) extended their previous technique to 2-dimensional case so as to obtain the azimuthal dependence of the wave.

Recently, simultaneous observations of ELF-VLF natural waves have been carried out at Syowa Station, Antarctica, and its geomagnetically conjugate stations in Iceland, *i.e.* Husafell, Tjörnes and Isafjörður (SATO *et al.*, 1984, MATSUDO and SATO, 1986). They reported the periodic VLF emissions ( $T=5.6$  s) in the frequency range from 1 to 1.7 kHz were observed simultaneously at these stations and there was a slight difference in the emission intensities observed at the three stations in Iceland. It seems to be highly probable that these emissions have propagated to the ionosphere through a duct in the magnetosphere.

In order to find a theoretical support to these experimental results of multi-station observations, the distributions of the amplitude and polarization of the VLF wave on the ground are calculated in this paper using the full wave technique (described in paper 1) under the condition that the downgoing whistler waves are emitted from a duct. In this calculation, the width of the transmission cone is kept constant while the width of the trapping cone is varied, and a nighttime ionosphere model is used, which is based on an actual rocket observation in high latitude (LERFALD and LITTLE, 1970) is used.

## 2. Model for Calculation

There are three types of whistler mode wave propagation between both the hemispheres (TIXIER and CHARCOSSET, 1978): (1) ducted propagation (2) nonducted propagation, and (3) partly ducted propagation. In this paper, whistler mode waves are

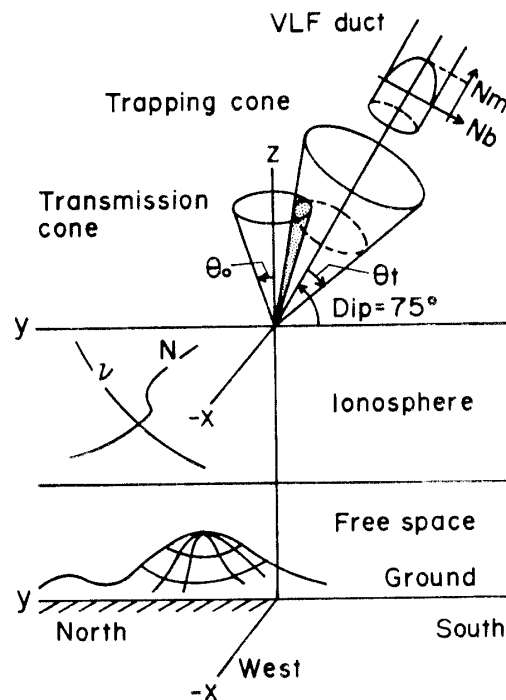


Fig. 1. A schematic illustration of the problem. The transmission cone and the trapping cone are assumed in this paper to be at the altitude of 150 km. The width of the transmission cone is  $5.0^\circ$  in our calculation model.

assumed to propagate in a duct in the magnetosphere which is terminated at the lower ionosphere. The direction of the wave normal of these waves is uniformly distributed in the trapping cone. Snell's law requires that a downgoing whistler mode wave can reach the ground only when its wave normal lies within the transmission cone angle ( $\theta_0 = \sin^{-1} 1/n$ , where  $n$  is refractive index at the altitude of incidence which is taken to be 150 km in this paper). On the other hand, the trapping cone angle is given as follows under the condition of  $f/f_H \ll 1$ , where  $f$  is the whistler mode wave frequency of interest and  $f_H$  is the electron gyrofrequency.

$$\theta_T = \cos^{-1} N_b/N_m,$$

where  $N_b$  is the background electron density and  $N_m$  is the maximum electron density in the duct. The enhancement factor ( $E = N_m/N_b - 1$ ) is taken as an index which indicates the enhancement rate of the electron density in the duct.

Four cases are considered in the configuration of trapping cone with respect to the transmission cone at the termination of the duct at an altitude of 150 km as shown in Fig. 2. In cases (a) through (b), the axis of the trapping cone is parallel to the magnetic field line, and the width of the trapping cone is varied. The axis of the trapping cone lies in the geomagnetic meridian plane. According to the ray theory, a downgoing whistler wave with wave normal direction lying within the shaded area in Fig. 1 (the common area in the trapping and transmission cones), can penetrate the lower ionosphere.

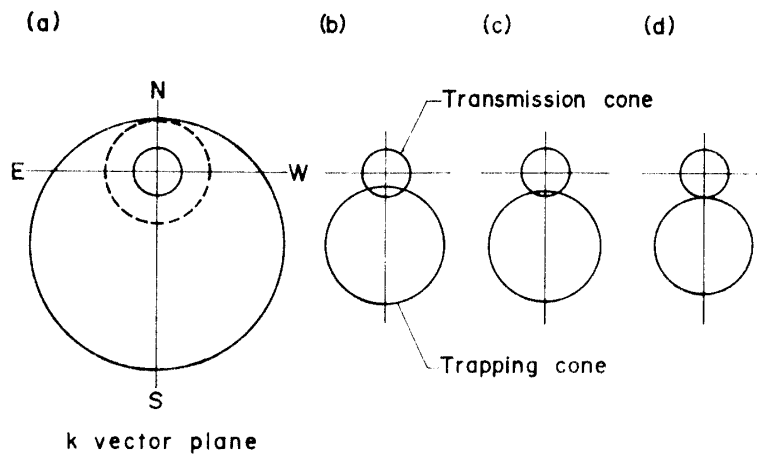


Fig. 2. Projection of the trapping and the transmission cones at the incident altitude of 150 km. The width of trapping cone in cases (a) through (d) are  $20^\circ$ ,  $12.5^\circ$ ,  $10.7^\circ$  and  $10^\circ$ , respectively, which correspond to the different enhancement factor values of the electron density in the duct, 10, 2.5, 1.8 and 1.5% respectively.

Figure 3 is the ionosphere model used in our numerical calculation. The electron density profile in this figure was obtained from a rocket experiment (LERFALD and LITTLE, 1970) in the northern auroral zone during a magnetically quiet time. An effective collision frequency profile used for our calculation is also shown by a broken line in this figure. The gyrofrequency and dip angle are taken as 1.54 MHz and  $75^\circ$ , respectively, which are typical values in the auroral zone. The frequency is selected

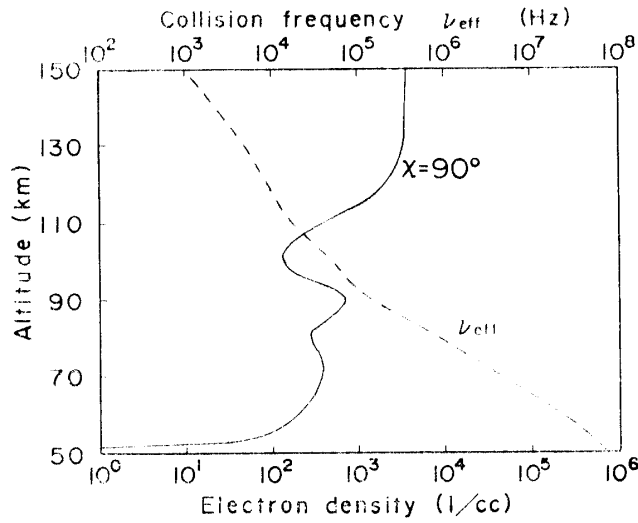


Fig. 3. The electron density and collision frequency profiles used in the numerical calculation.

as 1.5 kHz corresponding to the frequency band of VLF periodic emissions (SATO, 1984) and the conductivity and dielectric constant of the earth are selected as  $10^{-3}$  (S/m) and 10, respectively.

In our calculation a spatially confined electromagnetic wave is expressed by an infinite number of plane waves. A Cartesian coordinate system  $(x, y, z)$  is used as shown in Fig. 1. The electromagnetic field of the beam wave at an arbitrary altitude can be represented (NAGANO *et al.*, 1986) as:

$$\mathbf{e}(x, y, z) = (2\pi)^{-2} \iint G(k_x, k_y) \mathbf{F}(k_x, k_y, z) / E_y^{\text{R-DOWN}}(k_x, k_y, z=z_0) \cdot \exp(-j(k_x x + k_y y)) dk_x dk_y, \quad (1)$$

where  $G(k_x, k_y)$  is the Fourier component with  $k_x$  and  $k_y$  of the beam wave at the incident altitude and  $\mathbf{e}$  and  $\mathbf{F}$  are the column vector of the wave fields,  $E_x$ ,  $-E_y$ ,  $\mathcal{H}_x$  and  $\mathcal{H}_y$ . Their components consist of the full wave solutions in the original coordinate system for which  $k$  vector exists in  $x'-z'$  plane.  $\mathbf{F}$  is given by

$$\mathbf{F} = \begin{pmatrix} \sin \phi & \cos \phi & 0 & 0 \\ -\cos \phi & \sin \phi & 0 & 0 \\ 0 & 0 & \sin \phi & -\cos \phi \\ 0 & 0 & \cos \phi & \sin \phi \end{pmatrix} \begin{pmatrix} E_{x'} \\ -E_{y'} \\ \mathcal{H}_{x'} \\ \mathcal{H}_{y'} \end{pmatrix}, \quad (2)$$

where  $\phi$  is  $\tan^{-1} k_y/k_x$ .  $E^{\text{R-DOWN}}$  in eq. (1) is used to normalize the amplitude of  $-E_y$  at the incident altitude  $z_0$  to be unity and is calculated by the second row of eq. (2).

Since the calculation technique for eq. (1) is described in paper 1 in detail, we explain it briefly below;

(1) We choose  $G(k_x, k_y)$  which shows a uniform distribution within the trapping cone shown in cases (a) through (d) of Fig. 2. In these cases, the spectrum function  $G(k_x, k_y)$  depends on the width  $\theta_T$  of trapping cone, that is,

$$G(k_x, k_y) = \frac{\lambda_0^2}{\pi},$$

$$k_x^2 + (k_y - nk_0 \cos Dip)^2 \leq n^2 k_0^2 (\cos Dip - \cos (Dip + \theta_T))^2$$

$$G(k_x, k_y) = 0,$$

$$k_x^2 + (k_y - nk_0 \cos Dip)^2 > n^2 k_0^2 (\cos Dip - \cos (Dip + \theta_T))^2,$$

where  $\lambda_0$  and  $k_0$  are a wavelength and a propagation constant in free space, respectively, and  $n$  is a refractive index at the incident altitude. If we consider the downgoing whistler wave with the width  $\theta_T$  of the trapping cone, whose amplitude shows a gaussian distribution with a factor  $\sigma$ , where  $\sigma$  is defined by the distance in km from the point of maximum amplitude to the points of amplitude equal to  $e^{-1/2}$  times the maximum value; the waves with the spectrum function  $G(k_x, k_y)$  for cases (a) to (d) correspond to the gaussian beam waves with the width of 11.5, 24.1, 28.8 and 30.3 km, respectively.

(2) Equation (1) is approximated by a sum of a finite number of  $(k_x, k_y)$ , up to a few thousand components by using the Fast Fourier Transform algorithm, instead of integrating over an infinite number of  $(k_x, k_y)$ . We use the two dimensional FFT for  $2^7 \times 2^7$  data points. The spatial resolution on the ground is  $\lambda_0/16$  where  $\lambda_0$  is a wavelength in free space. For each elementary wave with  $k_x$  and  $k_y$ , we can use a full wave solution obtained by the multi-layered method taking account of the ground reflection effect (NAGANO *et al.*, 1975).

### 3. Calculated Results and Discussions

Figures 4a through 4d show the field intensities and polarizations over the area of  $1000 \times 1000$  km on the ground in cases of the downgoing whistler waves corresponding to (a) to (d) in Fig. 2, incident above the ionosphere at an altitude of 150 km. The maximum value of the field intensity on the ground is shown in dB at the bottom corner in every figure, where 0 dB is taken as  $1 \mu\text{V/m}$  when the Poynting flux of the downgoing wave at the incident altitude is  $1 \text{ pW/m}^2$ . The contour lines in Figs. 4a through 4d are drawn every 2 dB and denote the relative value to the maximum intensity in each figure. The center of each figure is the point where the signal level of the incident wave is maximum at an altitude of 150 km. The polarization pattern is shown for the same area. The right- and left-handed polarizations of the horizontal magnetic field components are denoted by solid lines and broken lines, respectively. The length of major axis in every elliptical polarization is taken as the same. As for the intensities of the received waves, they become smaller in the order of (a), (b), (c) and (d), because the number of the elementary downgoing waves within the transmission cone decreases in the same order. However, case of (d) with no wave in the transmission cone, a wave with relatively strong amplitude can reach the ground as an evanescent wave, and this is worth noting. This is due to the fact that the propagation distance from the ionosphere to the ground is shorter than the wave length of the downgoing wave at 1.5 kHz. The shapes of equi-intensity the contour lines change from a circle to an ellipse elongated toward the north-south direction in the order of (a) to (d) and the waves in free space propagate northward by multiple reflections between the earth and the ionosphere as seen in Figs. 4b and 4c.

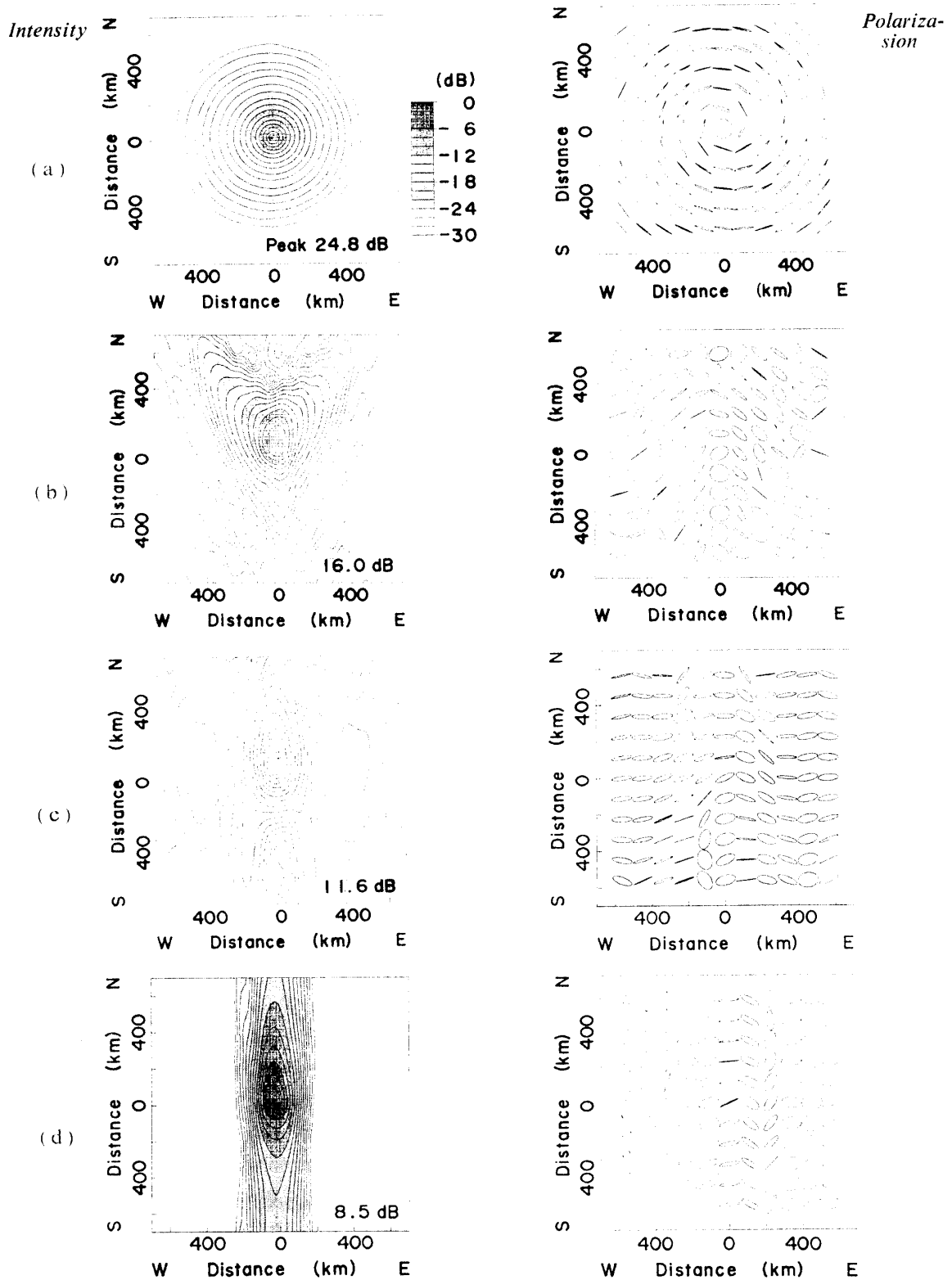


Fig. 4. The contour of the intensity of the wave magnetic field (left) and the polarization pattern (right) for the four cases of wave normal distribution shown in Fig. 2. The calculation is carried out at  $f=1.5$  kHz for the ionospheric model shown in Fig. 3. Intensity: The absolute maximum intensity is indicated at the right corner of the bottom of each figure, where 0 dB is taken as  $1 \mu\text{V}/\text{m}$  when Poynting flux of the downgoing whistler wave at the incident altitude is  $1 \text{ pW}/\text{m}^2$  and the contour lines are plotted every 2 dB attenuation. Polarization: Polarization patterns at every mesh point of 110 km interval. Solid and broken lines denotes the right- and left-handed polarizations, respectively.

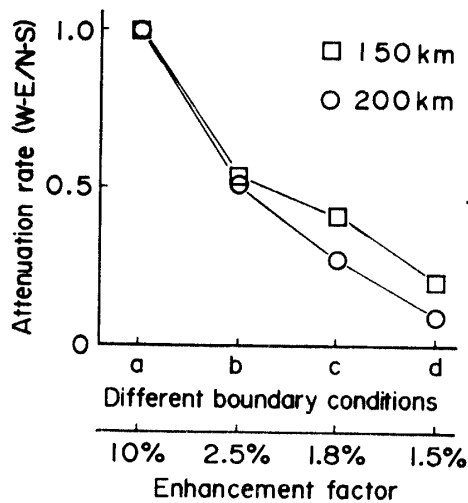


Fig. 5. The change of the ratio of the attenuation rate in the west-east direction and in the north-south direction measured at distances of 150 and 200 km from the point of maximum intensity for four different cases shown in Fig. 2.

Figure 5 shows a ratio of attenuation rate in the west-east and north-south directions at distances of 150 and 200 km from the maximum point of the intensity, for different boundary conditions of cases (a) to (d) in Fig. 2, with different enhancement factor values of the electron density in the duct, 10, 2.5, 1.8 and 1.5% respectively. If we can observe the attenuation ratio along the N-S and W-E direction at the distance of 150 or 200 km, we can estimate the enhancement factor of the duct by using the characteristics shown in Fig. 5 under an assumption that the observed fields consist only of downgoing waves propagating through a duct. As for the polarization patterns, the right handed nearly circular polarization can be seen within a distance of 100 km from the center in Fig. 4a and it abruptly changes to a linear polarization outside the circle of 100 km radius. However, in cases (b) through (d), the left-handed elliptical polarization appears at the region where the intensity is as strong as  $\sim -10$  dB of maximum intensity. The case like Fig. 4a is not likely to take place in middle latitudes because the dip angle becomes small so that the axis of the trapping cone is widely separated from the transmission cone. Therefore, the left-handed polarized wave may appear on the ground even when the amplitude of the wave is strong. In fact, OKADA and YAMAGUCHI (1985) have often observed the left-handed polarized whistler waves on the ground in middle latitudes.

#### 4. Concluding Remarks

The characteristics of the field intensity and polarization on the ground are obtained in the area of about  $1000 \times 1000$  km by a two dimensional full wave calculation for downgoing whistler mode waves injected from the magnetosphere into the Earth-ionosphere waveguide, where the incident wave normals are assumed to distribute uniformly over the transmission cone. The results we have obtained in this paper are as follows:

(1) When the transmission cone is within the trapping cone, the intensity of the wave on the ground decreases symmetrically with increasing distance from the maxi-

mum amplitude point. However, when the trapping cone is partly inside the transmission cone, the intensity characteristics are distorted toward the north direction and the intensity gradient in the west-east direction becomes steeper.

(2) The left-handed polarization appears even in the region where the intensity is strong when the trapping cone is partly inside the transmission cone.

(3) The numerical results of the amplitude distribution strongly suggest that the enhancement factor of electron density in the duct can be estimated from the ratio of spatial attenuation rate of the field intensities on the ground in the N-S and E-W directions.

(4) The exit point of the downgoing whistler wave at the bottom of the ionosphere can be estimated from the ratio of wave intensities observed by multiple stations on the ground.

Finally, we can expect that the calculation results in this paper will be useful in deciding a spatial separation of the station network for ELF-VLF ground observations.

#### Acknowledgments

The authors wish to express their thanks to Prof. M. EJIRI, Dr. N. SATO and Mr. H. YAMAGISHI for their support to this study. This research was partially supported by the Grant-in-Aid for research from the Ministry of Education, Science and Culture, Japan (No. 61550238).

#### References

- BUDDEN, K. G. (1961): *Radio Wave in the Ionosphere*. London, Cambridge Univ. Press, 482 p.
- HELLIWELL, R. A. (1965): *Whistler and related ionospheric phenomena*. Stanford, Stanford Univ. Press, 349 p.
- LERFALD, G. M. and LITTLE, C. G. (1970): *D-region electron temperatures at the northern auroral zone*. *Radio Sci.*, **5**, 1017–1028.
- MACHIDA, S. and TSURUDA, K. (1984): *Intensity and polarization characteristics of whistlers deduced from multi-station observations*. *J. Geophys. Res.*, **89**, 1675–1682.
- MATSUDO, T. and SATO, N. (1986): *Short-period magnetic pulsations induced by periodic VLF emissions*. *Mem. Natl Inst. Polar Res., Spec. Issue*, **42**, 1–9.
- NAGANO, I., MAMBO, M., and HUTATSUISHI, G. (1975): *Numerical calculation of electromagnetic waves in anisotropic multilayered medium*. *Radio Sci.*, **10**, 611–617.
- NAGANO, I., MAMBO, M., YOSHIZAWA, S., KIMURA, I. and YAMAGISHI, H. (1982): *Full wave calculation for a gaussian VLF wave injection into the ionosphere*. *Mem. Natl Inst. Polar Res., Spec. Issue*, **22**, 46–57.
- NAGANO, I., MAMBO, M., SHIMBO, T. and KIMURA, I. (1986): *Intensity and polarization characteristics along the earth's surface for the ELF-VLF waves emitted from a transmission cone in the high latitude*. *Mem. Natl Inst. Polar Res., Spec. Issue*, **42**, 34–44.
- OKADA, T. and YAMAGUCHI, T. (1985): *Moshiri ni okeru sasen henpa hoissurâ no kansoku (Observation of left-handed polarized whistlers at Moshiri)*. *Trans. IECE Jpn.*, **J68-B**, **11**, 1321–1322.
- PITTEWAY, M. L. V. and JESPERSEN, J. L. (1966): *A numerical study of the excitation, internal reflection and limiting polarization of whistler waves in the lower ionosphere*. *J. Atmos. Terr. Phys.*, **28**, 17–43.
- SATO, N. (1984): *Short-period magnetic pulsations associated with periodic VLF emissions ( $T \sim 5.6$  s)*. *J. Geophys. Res.*, **89**, 2781–2787.



- SATO, N., FUKUNISHI, H. and SAEMUNDSSON, Th. (1984): Operation plan for the Iceland-Syowa conjugate campaign in 1983-1985. Mem. Natl Inst. Polar Res., Spec. Issue, **31**, 169-179.
- TIXIER, M. and CHARCOSSET, G. (1978): Partly ducted whistlers over Europe. J. Atmos. Terr. Phys., **40**, 601-613.
- TSURUDA, K. (1973): Penetration and reflection of VLF waves through the ionosphere; Full wave calculations with ground effect. J. Atmos. Terr. Phys., **35**, 1377-1405.
- TSURUDA, K., MACHIDA, S., TERASAWA, T., NISHIDA, A. and MAEZAWA, K. (1982): High spatial attenuation of the Siple transmitter signal and natural VLF chorus observed at ground-based chain stations near Roberval, Quebec. J. Geophys. Res., **87**, 742-750.

*(Received Junly 20, 1986; Revised manuscript received November 25, 1986)*